AFRL-RD-PS
TP-2010-1023

THE AGGREGATE BEHAVIOR OF BRANCH POINTS- ALTITUDE AND STRENGTH OF ATMOSPHERIC TURBULENCE LAYERS: POSTPRINT

Denis W. Oesch, et al.

Air Force Research Laboratory
3500 Aberdeen Ave SE
Kirtland AFB, NM 87117

01 June 2010

Technical Paper

AIR FORCE RESEARCH LABORATORY
Directed Energy Directorate
3550 Aberdeen Ave SE
AIR FORCE MATERIEL COMMAND
KIRTLAND AIR FORCE BASE, NM 87117-5776

REPORT DOCUMENTATION PAGE

Form Approved
OMB No. 0704-0188

1. REPORT DATE *(DD-MM-YYYY)*	2. REPORT TYPE	3. DATES COVERED *(From - To)*
01-06-2010	Technical Paper	Oct 1, 2008- Jun 1, 2010

4. TITLE AND SUBTITLE
The Aggregate Behavior of Branch Points- Altitude and Strength Of Atmospheric Turbulence Layers: Postprint

5a. CONTRACT NUMBER
In House DF702151

5b. GRANT NUMBER

5c. PROGRAM ELEMENT NUMBER
62890F

6. AUTHOR(S)
*Denis W. Oesch, Darryl J. Sanchez, Carylong M. Tewksbury-Christle, Patrick R. Kelly

5d. PROJECT NUMBER
2301

5e. TASK NUMBER
SJ

5f. WORK UNIT NUMBER
41

7. PERFORMING ORGANIZATION NAME(S) AND ADDRESS(ES)

Air Force Research Laboratory
3550 Aberdeen Ave SE
Kirtland AFB, NM 87117

Science Applications International
2109 Airpark Road Southeast
Albuquerque, NM 87106-3236

8. PERFORMING ORGANIZATION REPORT NUMBER

9. SPONSORING / MONITORING AGENCY NAME(S) AND ADDRESS(ES)

Air Force Research Laboratory
3550 Aberdeen Ave SE
Kirtland AFB, NM 87117

10. SPONSOR/MONITOR'S ACRONYM(S)
AFRL/RDS

11. SPONSOR/MONITOR'S REPORT NUMBER(S)
AFRL-RD-PS-TP-2010-1023

12. DISTRIBUTION / AVAILABILITY STATEMENT

Approved for Public Release

13. SUPPLEMENTARY NOTES
Accepted for publication in the SPIE annual conference; August 2010; San Diego, CA. 377ABW-2010-1136, July 12, 2010. "GOVERNMENT PURPOSE RIGHTS"

14. ABSTRACT

In earlier work we have shown that pupil plane branch points carry information about the conditions of the atmospheric turbulence. Experiments in the Atmospheric Simulation and Adaptive-optic Laboratory Test-bed (ASALT) at the Air Force Research Laboratory. Directed Energy Directorate's Starfire Optical Range have shown that branch points can provide the number and velocity of turbulence layers. Here we demonstrate that these measurements can further be used to estimate the turbulence layers' altitude and strength. This work is the culmination of research demonstrating that a methodology exists for identification of the number, altitude, strength, and velocity of atmospheric turbulence layers.

15. SUBJECT TERMS

16. SECURITY CLASSIFICATION OF:			17. LIMITATION OF ABSTRACT	18. NUMBER OF PAGES	19a. NAME OF RESPONSIBLE PERSON
a. REPORT	b. ABSTRACT	c. THIS PAGE			Patrick Kelly
Unclassified	Unclassified	Unclassified	SAR 1	18	19b. TELEPHONE NUMBER *(include area code)* 505-846-2094

Standard Form 298 (Rev. 8-98)
Prescribed by ANSI Std. 239.18

This page is intentionally left blank.

The Aggregate Behavior of Branch Points - Altitude and Strength of Atmospheric Turbulence Layers

Denis W. Oesch[a], Darryl J. Sanchez[b], Carolyn M. Tewksbury-Christle[b], Patrick R. Kelly[b]

[a]Science Applications International Corporation, Albuquerque, New Mexico, USA

[b]Starfire Air Force Research Laboratory, Directed Energy Directorate, Kirtland Air Force Base, New Mexico, USA

ABSTRACT

In earlier work we have shown that pupil plane branch points carry information about the conditions of the atmospheric turbulence. Experiments in the Atmospheric Simulation and Adaptive-optic Laboratory Test-bed (ASALT) at the Air Force Research Laboratory, Directed Energy Directorate's Starfire Optical Range have shown that branch points can provide the number and velocity of turbulence layers. Here we demonstrate that these measurements can further be used to estimate the turbulence layers' altitude and strength. This work is the culmination of research demonstrating that a methodology exists for identification of the number, altitude, strength, and velocity of atmospheric turbulence layers.

Keywords: branch points, density, atmosphere, turbulence, adaptive optics

1. INTRODUCTION

In classical adaptive optical systems, branch points in the wave front sensor (WFS) measurement only serve to degrade system performance. Branch points and their ramifications for adaptive optics are detailed by Fried.[1-3]

The Atmospheric Simulation and Adaptive-optics Laboratory Team (ASALT) has been studying the behavior of pupil plane branch points. We have presented results from our laboratory experiments which show[4] that pupil plane phase measurements can be used to identify groups of branch points having a common velocity. This measured velocity scales to the velocity of the turbulence layer responsible for the formation of those branch points. Under the assumption of unique turbulence layer velocities, the number of sets of branch points identified through this method identifies the number of turbulence layers. Further we demonstrated,[5] that within the constraints of our atmospheric turbulence simulator (ATS),[6] the branch point density from a single turbulence layer follows a well defined empirical function dependent on the strength of and distance to the turbulence layer.

These four parameters; strength, distance, velocity and number, characterize the three dimensional layered atmospheric model. Velocity and number are handled fairly effectively with the isolation of pupil plane branch point motion. However, strength and distance are tied together in branch point density. Some of our other work has shown that branch point separation similarly depends on the strength and distance of the atmospheric turbulence layer. Branch point separation is a measure of the distance between two branch points of opposite sign that are connected by a 2π discontinuity in the measured phase; a branch point pair. These relationships offer the possibility that density and separation may combine to give us a means of estimating the strength and distance parameters.

In this paper we will show the dependence of branch point separation on the strength and distance of a single turbulence layer in our ATS. We will begin with a brief discussion on our experimental set-up and look at the results of our previous work on branch point density. Then to begin our discussion on branch point separation, in Section 3 we will detail the process through which we identify persistent pairs in the WFS measurements. Persistent pairs are those points which remain paired through time in the WFS data. Next we will discuss the application of this technique to experimental data examining the behavior of this measured separation as a function of strength and distance of an atmospheric turbulence layer in Section 4. Finally, in Section 4.4 we will investigate the use of the empirical relationships for branch point density and separation in estimating the strength and distance of the layer, followed by a discussion of the results in Section 5.

2. BACKGROUND

The ATS that provides the turbulence for the ASALT adaptive optical systems creates a one or two layer atmosphere where the standard parameters, r_0, Rytov and f_G are controllable and repeatable. All of the data presented here was collected using 1.55 μm light with a high resolution (256x256 pixel) temporal SRI, scaled to a 1.5 meter aperture. The system consists of two phase screens inscribed with a Kolomogorov structure. The placement of these screens selects the r_0 and Rytov parameters for the atmospheric turbulence. Rotating the phase screens provides simulated wind speed for each layer. This type of simulator models Taylor's frozen flow-type turbulence.

Added to this standard ATS is an optical trombone. This simple addition consists of a collection of turning flats, two of which sit on a sliding mount that allows for the addition of propagation distance between the phase screens and the adaptive optical system. Increasing the propagation distance raises the Rytov parameter for a given turbulence strength. At the same time the addition of the trombone moves the location of the relayed pupil providing a larger range of r_0's than can be simulated by the ATS alone.

In the ATS, the strength of the phase screens is set by an inscribed coherence length, $r_{0_{PW}}$, based on the prescription for the screen's design. The turbulence strength simulated by a single phase screen, at altitude $z = z_1$, is given by

$$C_n^2(z_1) = \frac{6.88}{2.91}\left(\frac{Dr_{0_{PW}}}{d_{pw}}\right)^{-5/3} k_0^{-2}. \tag{1}$$

Here D represents the size of the aperture the system is modeling while d_{pw} is the beam size of the light incident on the phase screen. k_0 is the wave number. Since C_n^2 is only a delta function in z, the corresponding pupil plane r_0 is simply

$$r_0 = \left(\frac{2.91}{6.88} C_n^2(z_1) k_0^2\right)^{-3/5}. \tag{2}$$

Given this relationship between $C_n^2(z)$ and r_0 it is easy to talk in terms of only r_0 when discussing the strength of the ATS turbulence. For this paper, the strength of the turbulence will be given in terms of the corresponding r_0.

Using a temporal SRI we collect a series of phase measurements, or frames of WFS data, following the evolution of the turbulence in time. These time resolved measurements of the optical wave in the pupil plane track the behavior of the branch points. Given sufficient turbulence strength and propagation distance branch points form at Rytov > 0.1. Branch points result from interference effects within the traveling optical wave and their locations are associated with zeros in the amplitude and circulations in the phase. The sign of the circulation, positive or negative, is considered the polarity of the branch point. Branch points are located with elementary circulations in the $mod_{2\pi}$ phase, that is $2x2$ regions of the WFS frame are used to estimate the sum of the gradients about each intersection of grid lines in the phase data. Identification of branch points in the measured phase is detailed fully in our paper on density.[5]

2.1 Branch Point Density

The density of branch points, ρ_{BP}, is the average number of circulations detected per frame of phase data divided by the area of the system aperture, which in this case, is scaled to simulate a 1.5 meter system. From our ASALT measurements[5] using a single phase screen of the ATS, we determined an empirical relationship between the branch point density and the distance and strength of the atmospheric layer given by

$$\rho_{BP_{emp}} = C_\rho k_0^{-5/6} r_0^{-11/3} z_0^{-1} (z - z_0)^{11/6} \tag{3}$$

with k_0 the wave number and C_ρ as a scaling constant, found to be 0.747. z is the altitude of the turbulence layer above the pupil plane and r_0 is the Fried parameter. z_0 was identified as the threshold distance at which branch

points begin to form. This is determined for each configuration using the equation for the Rytov parameter, σ_χ^2, for a single turbulence layer,

$$\sigma_\chi^2 = 0.5631(\frac{6.88}{2.91})k_0^{-5/6}r_0^{-5/3}z^{5/6}. \quad (4)$$

Setting $\sigma_\chi^2 = 0.1$, the point at which branch points are known to begin to form, and solving for the distance, z as the threshold distance, z_0, gives

$$z_0 = 0.0448k_0r_0^2. \quad (5)$$

3. PAIRING ALGORITHM

In order to discuss a relationship between branch point separation and the strength and distance of a turbulence layer, it is necessary to first establish the separation of branch point pairs as a meaningful parameter. In this section we discuss our technique for the identification of persistent pairs in the WFS data in order to attribute those pairs to a specific turbulence layer.

The circulation about every branch point includes a 2π discontinuity in the measured phase extending outward from the branch point. Two branch points of opposite polarity can be paired off such that they share a single discontinuity referred to as a branch cut. In $mod_{2\pi}$ phase data, as is captured with a temporal SRI, branch cuts between pairs of points can get mixed up with the 2π discontinuities due to phase wrapping, leading to ambiguity in how branch points should be paired for two-dimensional phase unwrapping.[7]

The procedure that follows looks to isolate branch point pairs by following the frequency with which they pair in time by constructing from a time resolved phase measurement of the optical wave the connections that bind pairs of branch points together throughout the measurement as persistent pairs. Ultimately it is the behavior of these persistent pairs, through their mean separation, that we'll be studying in relation to the strength and distance of the turbulence layer.

3.1 Process Overview

Our pairing algorithm follows five basic steps starting from WFS data comprised of multiple frames of $mod_{2\pi}$ phase; (1) identification of branch points, (2) estimation of group velocities, (3) initial 2-D pairing, (4) enhanced 2-D pairing and (5) velocity filtering for persistent pairs. These steps are shown at a cartoon level in Figure 1. After identification and estimation of velocity, each step will be detailed in the following sections. Here we just give an overview of the algorithm to set the stage for the discussion of the later sections.

Given measured phase data of $MxNxP$ dimensions, where MxN is $256x256$ for our temporal SRI and P is the number of consecutive frames collected, we begin by creating a polarity array of $(M-1)x(N-1)xP$ zeros. The reduction in size is a by product of how we locate the branch points in phase data. Using elementary circulations around 2x2 regions, identified branch points are assigned to the intersection of the grid lines within the $2x2$ region, thus the final collection of possible positions occupy an array of the reduced size relative to the original phase data. This array is represented in Figure 1(a).

For each frame of phase data, circulations are located, and a ± 1 is placed in the corresponding position in the polarity array signify and positive or negative circulations of 2π. The location of positive and negative circulations are shown as red and green dots in Figure 1(b).

For every point in the polarity array an instantaneous velocity vector, $\Delta x/\Delta t\hat{i} + \Delta y/\Delta t\hat{j}$, is calculated with respect to every other point of like polarity throughout the $(M-1)x(N-1)xP$ array. A two dimensional distribution of all possible velocity components reveals strong correlations that appear as peaks, signifying the actual velocities of the branch point groups.[4] The estimated instantaneous velocity vectors for the positive circulations are shown in Figure 1(c) in purple.

With the locations of the individual branch points known, an initial pairing is done that identifies tentative branch point pairs using a standard walking algorithm, see Figure 1(d). The process is to simply follow the branch cut from one branch point to its partner. However, as there is no difference between 2π discontinuities formed from branch point phase and those due to wrapping effects, a secondary process is used to enhance the identification of branch cuts. This additional process is done by varying the piston component of the measured

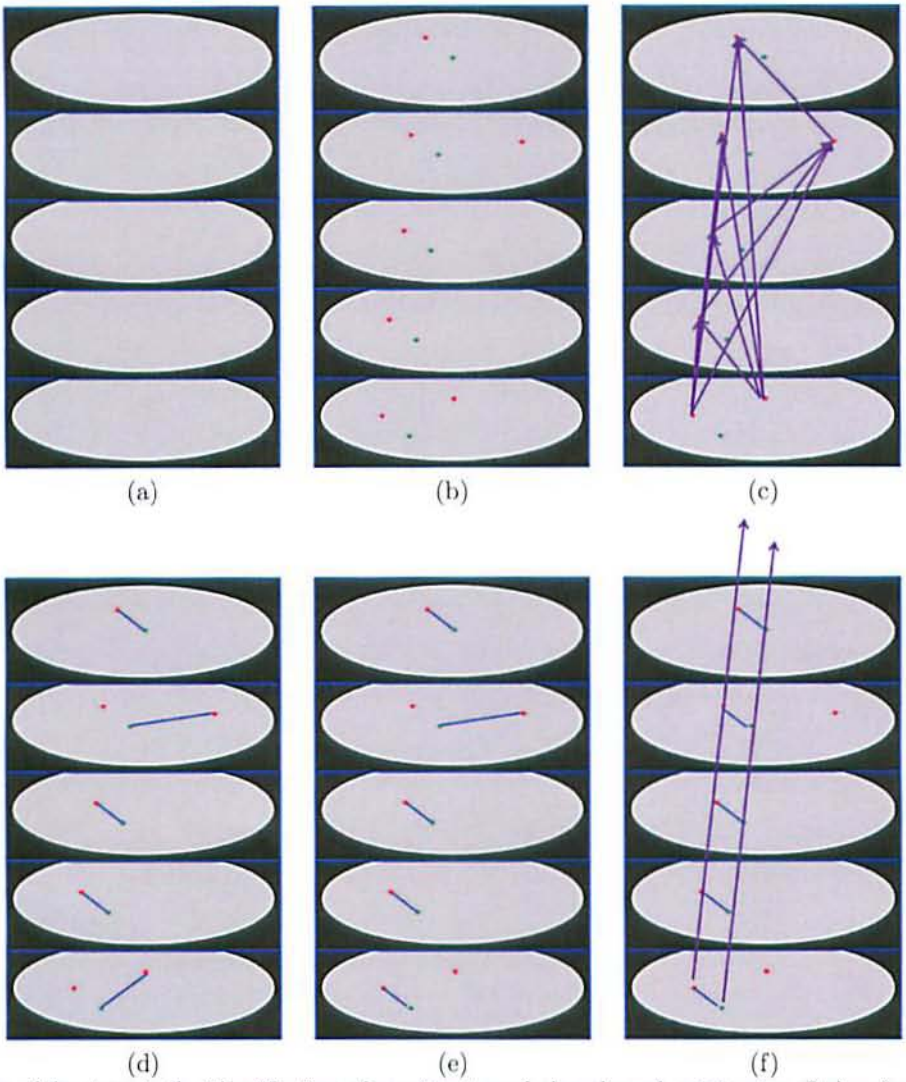

Figure 1. *Cartoon of the steps in the identification of persistent pupil plane branch point pairs. Red and green dots indicate the positive and negative circulations respectively. (a) The empty polarity array. (b) The polarity array with ± 1's at the locations of positive and negative circulations respectively. (c)Diagram showing the estimated velocities from the positive branch point locations. (d)Blue lines indicate the initial pairings following frame by frame use of a walking algorithm. (e)Pairings following the use of piston shifting technique. (6)Overlay of measured velocity to incorporate 3rd dimension of WFS data.*

phase. Each value of added piston repositions the 2π discontinuities due to wrapping, giving a different view of the branch cuts. So by filtering the branch point pairs according to their frequency improves the identification of pairs that may have been obscured by wrapping discontinues.

Finally the piston enhanced branch point pairs are filtered against the measured velocity vectors to identify pairs that repeat through the WFS data. This provides a means to track branch point pairs through time as well as the ability to separate branch points according to their turbulence layer.

3.2 Initial 2-D pairing

The pairing process begins with a typical frame by frame approach using a walking algorithm to follow the branch cuts from one branch point to the next. Isolating the branch cuts from phase data simplifies the work of

the walking algorithm by creating a 2-D map of the possible paths between branch points. We've developed a simple modification to the elementary circulation technique used for identifying branch points that also isolates all 2π discontinuities in the phase data.

3.2.1 The Difference of Gradients

When using an elementary circulation to interrogate the gradients in the phase, ϕ, about a $2x2$ loop in the identification of branch points in discrete data, what is really being identified is the branch cut emanating away from a branch point within the loop. That is to say that one of the four gradients computed from that $2x2$ region crosses over a 2π discontinuity and thus the sum of the gradients is $\pm 2\pi$. However if you were to compute the sum of the gradients around the same loop in $mod_{2\pi}$ the sum of the gradients would always be zero. This is because the 2π discontinuity only exists because the data is wrapped in $mod_{2\pi}$ but the sum of the gradients about the loop is not.

Therefore, if instead of looking for branch points through summing the gradients about closed loops, we look for differences between the x and y gradients normally

$$\begin{aligned} \delta x_{i,j} &= sign(\phi_{i,j} - \phi_{i+1,j}) \\ \delta y_{i,j} &= sign(\phi_{i,j} - \phi_{i,j+1}), \end{aligned} \tag{6}$$

versus $mod_{2\pi}$

$$\begin{aligned} \delta ex_{i,j} &= sign(mod_{2\pi}(\phi_{i,j} - \phi_{i+1,j})) \\ \delta ey_{i,j} &= sign(mod_{2\pi}(\phi_{i,j} - \phi_{i,j+1})), \end{aligned} \tag{7}$$

and we find that their signs are reversed in the presence of a branch cut. This leads to a simple process for reducing a frame of $mod_{2\pi}$ phase data to a map of 2π discontinuities. The signs of the gradients match in the absence of discontinuities, so their difference is zero. However, they are opposed when a discontinuity is present and their difference combines.

Using only the signs, $\pm$, of the gradients and dividing by the differences by 2,

$$\begin{aligned} \Delta x_{i,j} &= (\delta x_{i,j} - \delta ex_{i,j})/2 \\ \Delta y_{i,j} &= (\delta y_{i,j} - \delta ey_{i,j})/2, \end{aligned} \tag{8}$$

creates two sets composed only of discrete delta functions at positions of discontinuities. These sets by the nature of the differences are 256x255 and 255x256 for x and y respectively from a 256x256 frame of data. Shifting and adding the absolute values of these sets in the appropriate fashion,

$$BC_{i,j} = |\Delta x_{i,j}| + |\Delta x_{i+1,j}| + |\Delta y_{i,j}| + |\Delta y_{i,j+1}|, \tag{9}$$

creates a map containing all of the 2π discontinuities present in the phase data as shown in Figure 2

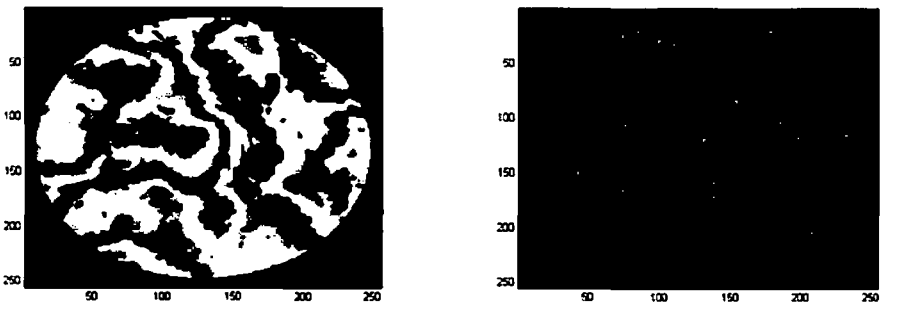

(a) (b)

Figure 2. *Sample WFS phase (left) and map of discontinuities from difference of gradients method (right).*

This map is then used with a typical walking algorithm approach to find branch point pairs. Starting from one branch point the algorithm simply follows the discontinuity until it locates a partner of opposite polarity. These two points are then considered a possible pair.

3.2.2 Piston Scanning

Unfortunately, due to wrapping discontinuities, not all of the branch points are connected in a single frame using the walking algorithm and difference of gradients method, see Figure 3. Here several branch point pairs have been highlighted in the insets to show how the discontinuities fell in the difference of gradient method. Sometimes the pair is clearly connected by a branch cut, Figure 3(a) and (b). However, wrapping discontinuities can interact with branch cuts in such a way as to obscure the branch cut, and in some cases even result in incorrect or missed pairings, Figure 3(c).

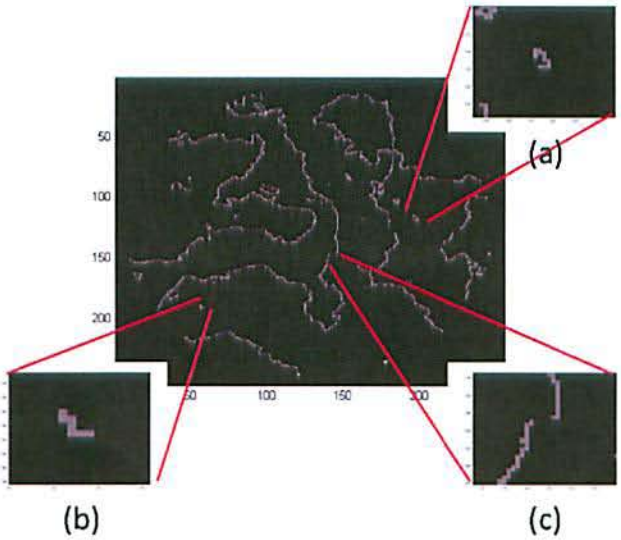

Figure 3. *Map of discontinuities from difference of gradients method with enlarged sections showing some of the branch point pairs and how the discontinuities are distributed around them.*

To improve the number of branch points paired within a given frame, we redistribute the wrapping discontinuities to better examine the branch cuts. The shape and number of wrapping discontinuities is set by the distribution of full optical wave when measured by the WFS. However there is an ambiguity in position due to unknown piston within the measurement.[8] Therefore, by adding piston to the $mod_{2\pi}$ phase we can redistribute the wrapping discontinuities to have a different view of the branch cuts according to

$$\phi_{\delta\phi} = mod_{2\pi}(\phi + \delta\phi). \tag{10}$$

We vary the added piston, applying the difference of gradients and looking for pairs with the walking algorithm each time, to create a collection of possible branch point pairings over the range of piston. In low density cases the branch points only pair with a single partner. In higher density regions, there may be two or more possible pairs for a single branch point. Therefore after determining all of the possible pairs from varying the piston, the pairings are filtered according to their frequency to isolate the most common pairs and eliminate pairs that aren't as well defined.

Overall this additional 2-D step increases the number of paired points in any given frame but doesn't remove the possibility of missing or incorrect pairs. To increase the number of high confidence pairs further we add in the measured velocity.

3.3 Velocity Filtering

Up to this point, all of the pairing has been applied on a frame by frame basis, with no regard for the time aspect of the WFS measurement. To begin we look at the polarity array now as a three-dimensional object, see Figure 4(a). Again, the red and green points indicate the positive and negative circulations respectively. The blue lines indicate where 2-D pairings have been identified. The common velocity component stands out strongly in this view of a sample of single layer turbulence. The close-up, Figure 4(b), reveals some of the issues discussed in the 2-D pairing sections.

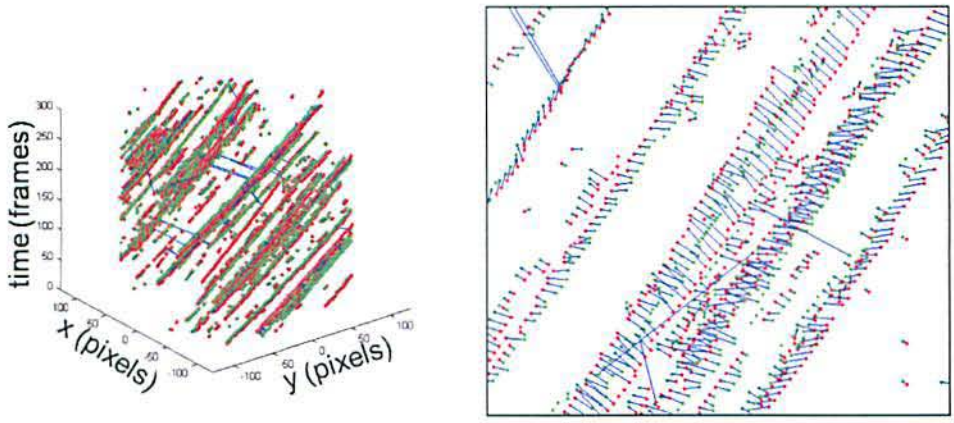

(a) (b)

Figure 4. *The polarity array shown in three dimenstions (left) a close-up of the array showing numerous 2-D only pairings (right)*

By comparing branch point pairs from frame to frame, we can filter the pairings according to their frequency of occurrences in time. Identifying those pairs that persist through time gives further confidence that these are correct branch point pairings. In Figure 5(a), the polarity array is shown after filtering the pairs by velocity. Immediately it can be seen that the long blue line segments of Figure 4(a), signifying incorrect pairings are gone. The close up in Figure 5(b) likewise shows a more orderly series of pairings than what was seen in Figure 4(b).

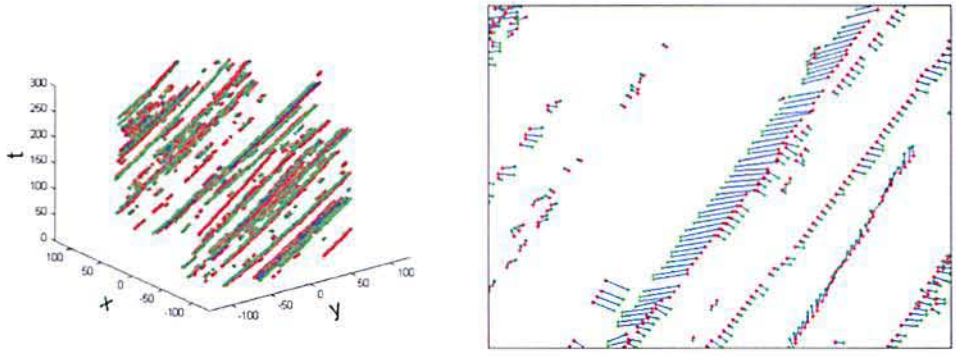

(a) (b)

Figure 5. *Collection of WFS frames as a 3D data set (left) and the associated polarity array (right)*

4. BRANCH POINT SEPARATION

It was hypothesized[9] that branch points form infinitesimally close together and then separate as the wave propagates. With the identification of persistent pairs in our WFS data it is natural to examine the behavior of

the separation of these pairs as a function of turbulence strength and distance. In what follows, we detail our experimental results over a range of turbulence conditions on the measured branch point separation.

4.1 Data and Methodology

For these test sequences, a single phase screen was used in conjunction with the optical trombone described in Section 2. In each data run, the strength of the turbulence is maintained while the distance to the phase screen is increased. This increase takes the form of eleven evenly spaced steps which covers a roughly 9 km range. For all of the turbulence strengths combined this provide a test region from 0 - 15 km. This independently varies the Rytov parameter from $0 - 1.2$, as shown in Figure 6. Between each data run, the turbulence strength, which in our test-bed is equivalent to varying r_0, is modified. In this way, eleven values of atmospheric strength were interrogated, ranging from 6.52 to 16.60 cm for a 1.5 meter aperture (see Table 1). For each trombone position

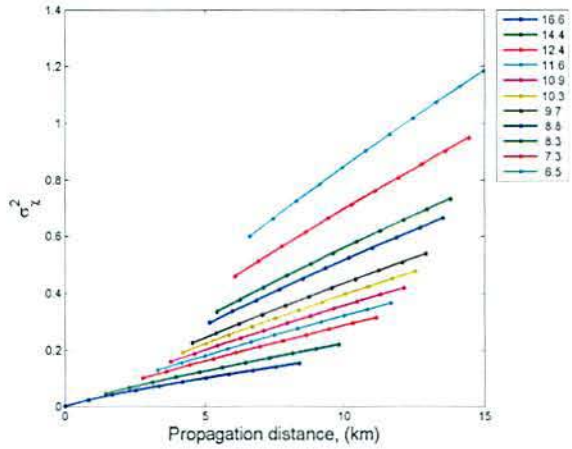

Figure 6. *Theoretical Rytov values for the single phase screen test configurations*

and turbulence strength, the phase screen was rotated at a constant speed for 200 frames. Data was collected for each configuration producing 200 - $256x256$ images of the phase for each of 121 turbulence conditions.

			ATS Configuration			Turbulence Conditions			
Ensemble Set #	Number of Realizations	Lens Set	Trombone Position (cm)	PW Position (low, high) (cm)	PW Step (low, high) (counts)	Propagation Range (km)	Turb. Velocity (low, high) (m/s)	r_0 (cm)	σ^2_χ
1	200	7	{0:5:50}	(106.3, *puck*)	(3, 0)	0.0-8.4	(11.75, 0)	16.6	0.00 – 0.15
2	200	7	{0:5:50}	(105.5, *puck*)	(3, 0)	1.5-9.8	(10.22, 0)	14.4	0.04 – 0.22
3	200	7	{0:5:50}	(104.5, *puck*)	(3, 0)	2.8-11.1	(8.79, 0)	12.4	0.10 – 0.32
4	200	7	{0:5:50}	(104.0, *puck*)	(3, 0)	3.3-11.7	(8.22, 0)	11.6	0.13 – 0.37
5	200	7	{0:5:50}	(103.5, *puck*)	(3, 0)	3.8-12.1	(7.71, 0)	10.9	0.16 – 0.42
6	200	7	{0:5:50}	(103.0, *puck*)	(3, 0)	4.2-12.6	(7.27, 0)	10.3	0.19 – 0.48
7	200	7	{0:5:50}	(102.5, *puck*)	(3, 0)	4.6-12.9	(6.87, 0)	9.7	0.23 – 0.54
8	200	7	{0:5:50}	(101.5, *puck*)	(3, 0)	5.2-13.5	(6.20, 0)	8.8	0.30 – 0.67
9	200	7	{0:5:50}	(101.0, *puck*)	(3, 0)	5.4-13.8	(5.91, 0)	8.3	0.34 – 0.73
10	200	7	{0:5:50}	(99.5, *puck*)	(3, 0)	6.1-14.4	(5.18, 0)	7.3	0.46 – 0.95
11	200	7	{0:5:50}	(98.0, *puck*)	(3, 0)	6.6-15.0	(4.61, 0)	6.5	0.60 – 1.19

Table 1. *Turbulence parameters used for measurement of branch point separation. For each Ensemble set, 200 frames of data was collected for each of 11 positions of the optical trombone, ranging in 5 cm increments from 0 to 50 cm. This corresponds to ranges of propagation distances and Rytov parameters for each Ensemble. The term 'puck' refers to the clear center portion of the phase screen. To be placed at 'puck' means the light was passing through the center of the screen and not contributing to the turbulence simulated by the ATS.*

4.2 Persistent Pair Separation

From each of the configurations on Table 1 a set of 200 frames of $mod_{2\pi}$ data was collected. The locations of all circulations were identified with separate polarity arrays. The group velocities were determined and persistent pairs identified. From the persistent pairs found, a single separation was calculated for each as the distance between paired points averaged over time. A single mean for each configuration was determined from the average of all of these persistent pair separations. This mean branch point separation, δP, is shown on Figure 7 versus modeled altitude. Each turbulence strength from Table 1 is represented by a different color and identified by the associated r_0 in the legend.

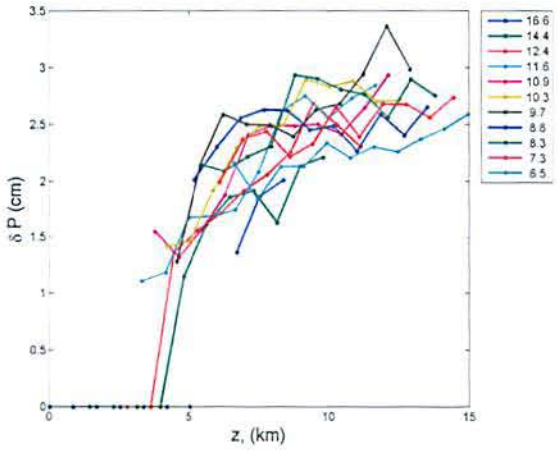

Figure 7. *Mean branch point separation from single phase screen data for selected turbulence strengths. For each curve, the turbulence strength, given by r_0, is held constant while the propagation distance is varied using the optical trombone.*

Following what was done with density, we begin by recasting Figure 7 in terms of the propagation distance beyond the branch point threshold, z_0 as given by Equation 5. This rescaling shown in Figure 8 reduces the spread of the separation curves similarly to what was seen for density.[5]

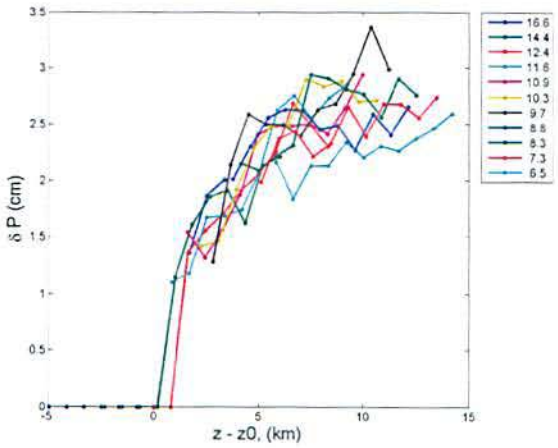

Figure 8. *Mean branch point separation vs distance beyond the branch point threshold, z_0.*

Unlike density, separation doesn't appear to have a strong dependence on the turbulence strength beyond

that of z_0. Recall that z_0 is dependent on k_0 and r_0^2.

4.3 Empirical Algebraic Form of the Branch Point Separation

Tatarskii[10] discussed attempts to determine a correlation radius of the intensity fluctuations for a horizontally propagating beam. He states that his experiments to estimate a mean size of the inhomogeneities in the intensity would always provide the same answer, $\sqrt{\lambda z}$. The mean size in his experiments can be thought of as an average distance between low intensity regions. These are the regions in which branch points are seen. Therefore it is a reasonable starting point for a functional relationship between branch point separation and distance. In Figure 9 each of the constant strength curves of Figure 8 are plotted separately in blue with a best fit curve based on the functional form of Tatarskii's mean correlation radius,

$$\delta P_{emp} = C_\delta \sqrt{\lambda(z - z_0)}, \tag{11}$$

in green. It is clear that this functional form is well suited to all of the configurations shown here with $C_\delta = 0.246$ which was determined through a least squares fit of all of the constant strength curves simultaneously. The data points outlined in red indicate those configurations which included a Rytov parameter greater than 0.4. This was the region at which the density appeared to saturate. Separation, however, doesn't begin to show possible saturation until further into the Rytov range. Though it is difficult to identify a single Rytov value at which this occurs from this data.

In this relationship, the strength of the turbulence determines the minimum propagation distance required for branch point pairs to form, but doesn't affect how they separate. Additionally the rate at which pairs of branch points move apart, the separation velocity, would appear to be only a function of the wavelength, given this equation. This aspect may provide additional information in future measurements.

4.4 Strength and Distance

Equation 11 relating mean separation of persistent pairs, δP, to the strength and distance of the turbulence layer is empirical. However, together with the relationship we determined for branch point density, ρ_{BP}, Equation 3, they present a means of determining additional characteristics of the atmospheric structure from branch point measurements. These two equations can be rewritten using the definition for z_0 (Equation 5) as

$$\rho_{BP_{emp}} = \bar{C}_\rho r_0^{-2} \left(\frac{z}{z_0} - 1\right)^{11/6} \tag{12}$$

and

$$\delta P_{emp} = \bar{C}_\delta r_0 \left(\frac{z}{z_0} - 1\right)^{1/2}, \tag{13}$$

where $\bar{C}_\rho = 0.0448^{5/6} C_\rho = 0.056$ and $\bar{C}_\delta = (0.0448(2\pi))^{1/2} C_\delta = 0.131$. Solving these equations for the strength, r_0 in terms of the branch point characteristics gives

$$r_0 = 2.24 \left(\frac{\delta P^{11}}{\rho_{BP}^3}\right)^{1/17}. \tag{14}$$

Then with Equation 5, we can identify the distance using

$$z = 2.61 k_0 \delta P^2 + z_0. \tag{15}$$

Using these equations then we can estimate the strength and distance of a single turbulence layer using pupil plane branch point measurements alone. For illustration purposes, this was done with the data collected from Table 1. Figure 10 shows the results.

This provide a verification of our empirical relationships rather than a demonstration of the technique given that this data is not independent of that used to to form the equations. In another paper, currently in preparation, we examine the use of this approach, along with measurements of the branch point motion, to determine the four parameters of a layered atmospheric model; number, velocity, strength and distance, using wave optics simulations.

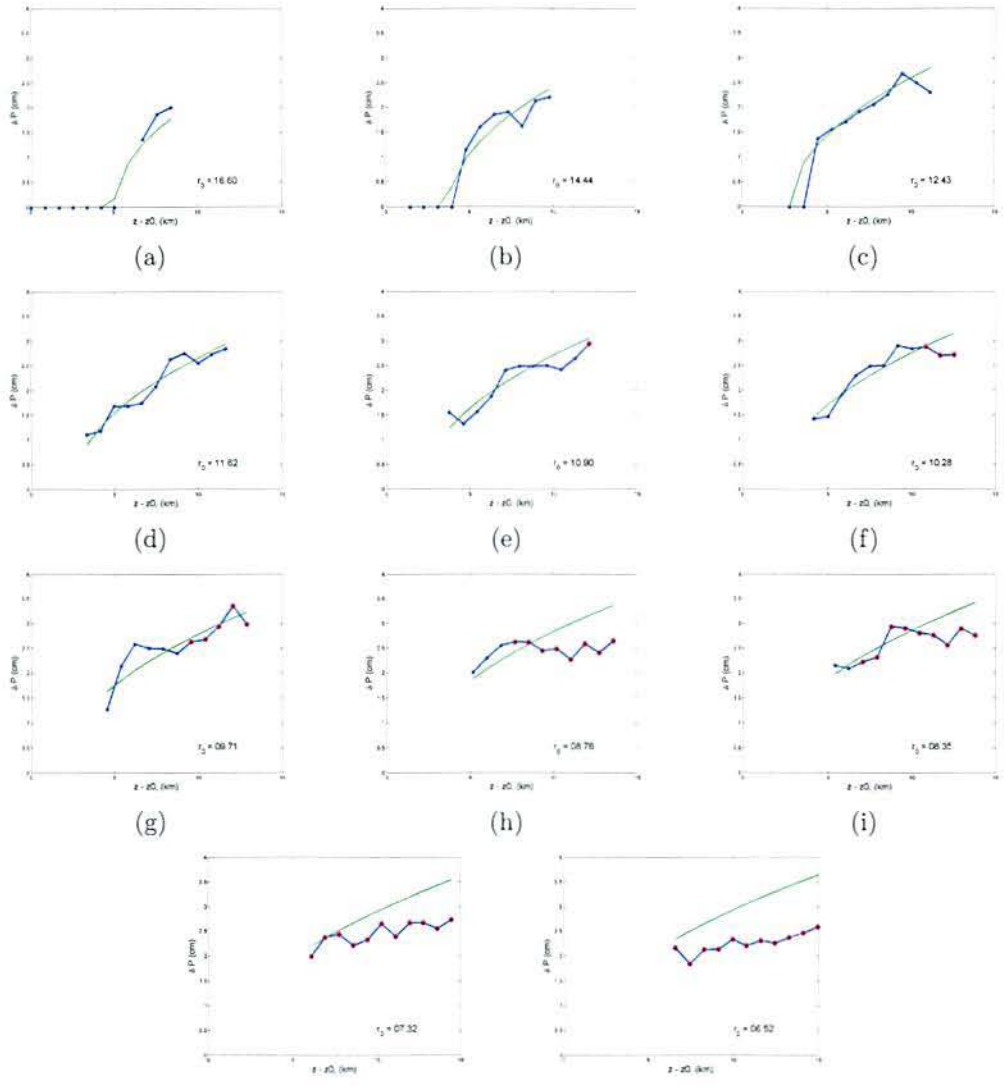

Figure 9. *Estimated mean branch point separation vs the mean separation predicted by the empirical form of Equation 11 for each of the tested r_0's. In each case the measured δP is plotted in blue while the empirically predicted value is plotted as a green curve. (a) $r_0 = 16.60cm$ (b) $r_0 = 14.44cm$ (c) $r_0 = 12.43cm$ (d) $r_0 = 11.62cm$ (e) $r_0 = 10.90cm$ (f) $r_0 = 10.28cm$ (g) $r_0 = 9.71cm$ (h) $r_0 = 8.76cm$ (i) $r_0 = 8.35cm$ (j) $r_0 = 7.32cm$ (k) $r_0 = 6.52cm$ Red circles indicate configurations where the Rytov parameter exceeds* 0.4. *Saturation doesn't appear to affect separation as it did density.*

5. DISCUSSION

We have demonstrated a method for determining a meaningful quantity from the separation of branch point pairs in WFS data. Our approach for isolating persistent pairs utilizing the temporal aspect of the phase measurement is a novel approach to characterizing the placement of branch cuts. It assumes a Taylor's frozen flow model for the underlying turbulence layers, this is the same as placing a lower limit on the sampling frequency of the wave front sensor measurement. The experimental results from a single turbulence layer, however, demonstrate the potential value of such a measurement. That a measurement of branch point separation for a single layer shows dependence on only the wavelength, distance and strength of the turbulence layer is significant.

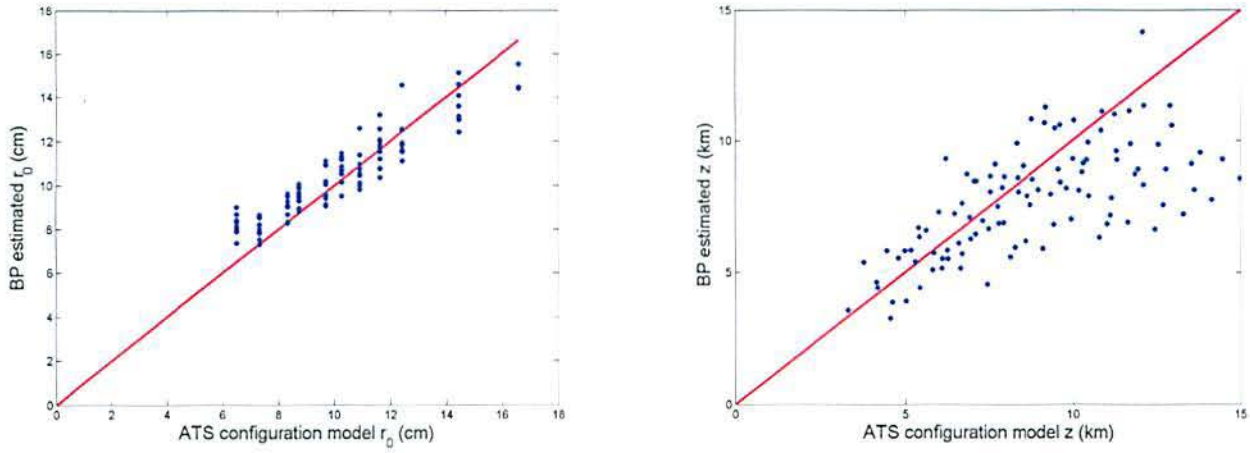

(a) (b)

Figure 10. *Using branch point measurements, density and separation, to estimate the turbulence layer strength and distance. (a) The estimated strength in terms or r_0 and (b) the estimated propagation distance versus the expected values, respectively for each, from the model used to set the ATS configuration parameters. The red lines indicate where perfect agreement between the estimated and predicted values should fall.*

Separation is the fourth parameter we have attributed to the information carried by branch points in WFS measurements. With the density, velocity and number of sets we've shown previously, these four branch point parameters provide a framework for the identification of the four characteristics of a layered model for atmospheric turbulence; number, velocity, distance and strength of the layers. Beginning with our earlier work on turbulence layer velocities from branch point measurements, it is possible to separate branch points into groups according to their associated turbulence layer by their velocities. The number of groups relates to the number of branch point producing turbulence layers with unique velocities. For each branch point group then, with the separation and density of that subset given by Equations 3 and 11, one would be able to determine the distance and strength of the identified layer. While these relationships are empirical they continue an effort to further characterize the nature of branch points in atmospheric turbulence and are giving insight into the underlying physics of branch point formation and propagation.

6. ACKNOWLEDGMENTS

We would like to express our gratitude to the Air Force Office of Scientific Research for their support in funding this research.

REFERENCES

1. D. L. Fried and J. L. Vaughn, "Branch cuts in the phase function," *Applied Optics* **31**, pp. 2865–2882, May 1992.
2. D. L. Fried, "Branch point problem in adaptive optics," *Journal of the Optical Society of America* **15**, pp. 2759–2768, October 1998.
3. D. L. Fried, "Crypto branch points: a problem in phase unwrapping," Tech Note TN-190, David Fried, February 2005.
4. D. W. Oesch, D. J. Sanchez, P. R. Kelly, K. P. Vitayaudom, C. M. Tewksbury-Christle, J. Smith, and N. E. Glauvitz, "The Aggregate Behavior of Branch Points: An Overview of Research in the ASALT lab," in *2009 DEPS Annual Conference*, D. Herrick, ed., Directed Energy Professional Society, 2009. Published in briefing format only.

5. D. W. Oesch, D. J. Sanchez, C. M. Tewksbury-Christle, and P. R. Kelly, "The Aggregate Behavior of Branch Points - Branch Point Density as a Characteristic of an Atmospheric Turbulence Simulator," in *2009 SPIE Annual Conference*, R. Carerras, T. Rhoadharmer, and D. Dayton, eds., SPIE, 2009.
6. S. V. Mantravadi, T. A. Rhoadarmer, and R. S. Glas, "Simple laboratory system for generating well-controlled atmospheric-like turbulence," in *Advanced Wavefront Control: Methods, Devices, and Applications II*, M. K. Giles, J. D. Gonglewshi, and R. A. Carerras, eds., *Presented at the Society of Photo-Optical Instrumentation Engineers (SPIE) Conference* **5553**, pp. 290–300, Oct 2004.
7. D. C. Ghiglia and M. D. Pritt, *Two Dimensional Phase Unwrapping: Theory, Algorithms, and Software*, John Wiley and Sons, Inc., New York, NY, 1998.
8. T. M. Venema and J. D. Schmidt, "Optical phase unwrapping in the presence of branch points," *Optics Express* **16**, pp. 6985–6998, May 2008.
9. D. J. Sanchez, D. W. Oesch, C. M. Tewksbury-Christle, and P. R. Kelly, "The Aggregate Behavior of Branch Points - The Creation and Evolution of Branch Points," in *2009 SPIE Annual Conference*, R. Carerras, T. Rhoadharmer, and D. Dayton, eds., SPIE, 2009.
10. V. I. Tatarskii, *The Effects Of Turbulent Atmosphere On Wave Propagation*, Israel Program for Scientific Translations Ltd., Jerusalem, 1971.

DISTRIBUTION LIST

DTIC/OCP
8725 John J. Kingman Rd, Suite 0944
Ft Belvoir, VA 22060-6218 1 cy

AFRL/RVIL
Kirtland AFB, NM 87117-5776 2 cy

Patrick Kelly
Official Record Copy
AFRL/RDSAE 1 cy

This page intentionally left blank.